ANEXO 4

“Multi component kinetic-spectrophotometric analysis. Selection of wavelength and time ranges.”

Hortensia Iturriaga, Jordi Coello, Santiago Maspoch and Marta Porcel

The Analyst, **126**, 1135, **2001**

FULL PAPER
THE ANALYST
www.rsc.org/analyst

Multi-component kinetic–spectrophotometric analysis. Selection of wavelength and time ranges

Hortensia Iturriaga, Jordi Coello, Santiago Maspoch* and Marta Porcel

Departament de Química, Facultat de Ciències, Universitat Autònoma de Barcelona, Unitat de Química Analítica, Edifici Cn, E-08193 Barcelona, Spain

Received 6th February 2001, Accepted 14th May 2001
First published as an Advance Article on the web 21st June 2001

An empirical method for the selection of the best wavelength and time ranges which can be used in the quantification of binary mixtures, in a kinetic–spectrophotometric system, is proposed. It is based on finding those ranges which provide the least correlation between the kinetic profiles and the spectra of the products of reaction. The method was applied to the analysis of binary mixtures using simulated data with different rate constant ratios and in the presence of an interference that shows spectral overlap with the analytes. Subsequently, the proposed method was applied to the resolution of dyphylline and proxyphylline mixtures. The system studied was characterized by an elevated similarity in the kinetic behavior of the analytes under pseudo-first-order conditions and an elevated degree of spectral overlap of the products of reaction. In spite of this, satisfactory results were obtained in the quantification of the two analytes. The standard error of prediction (SEP) and the standard deviation between replicates (SDBR) did not show significant differences, being of the order of 4 and of 3% for dyphylline and proxyphylline, respectively.

Introduction

Since the appearance of diode array spectrophotometers, which allow the complete registry of a UV–Vis spectrum in tenths of a second, and of multivariate calibration methods,[1] spectrophotometric resolution of mixtures has been converted into a routine analytical tool. The application of this methodology to kinetic–differential analysis[2] has considerably widened its analytical possibilities since the resolution can be performed on the basis of a spectral discrimination and also on basis of the different reaction rates, both aspects having a synergetic effect.

The application of conventional multivariate calibration techniques [*e.g.*, partial least squares (PLS)[3]] to spectral kinetic systems requires the unfolding of the intrinsically three-dimensional matrix (sample, wavelength, time) of the registered data in such a way that the scans recorded at various times are sequentially linked together to form a single row in the $\boldsymbol{X}$ data matrix, generating vectors ($\lambda_1 t_1$, $\lambda_2 t_1$, ..., $\lambda_p t_1$, ..., $\lambda_i t_j$, ..., $\lambda_1 t_k$, ..., $\lambda_2 t_k$, ..., $\lambda_p t_k$) of great length (easily of the order of 10 000 terms). It is evident that a great part of this information is very correlated and is redundant and that, in contrast, a certain number of variables cannot contain any type of useful information, which makes a previous selection of the variables advisable. By doing this, the precision of the results is improved.

In early work on wavelength selection in spectroscopic methods, Frans and Harris[4] demonstrated that the best precision could be obtained with a small number of variables, although that could lead to the loss of other interesting advantages of multivariate calibration.[1,3] Diverse variable-selection systems have been described, amongst which genetic algorithms[5–9] stand out owing to their great capacity. Nevertheless, the complexity of calculation and the need to have specific software available make their application difficult. On the other hand, the analyst generally has important previous information available in the resolution of mixtures using spectroscopic data, such as the spectrum of the products, for which, *a priori*, the spectral zones of maximum sensitivity for each analyte are already known. All of this means that, in practice, rather than searching for an optimal group of discrete variables, spectral modes and wavelength intervals are empirically selected.

This empirical methodology has been extended to kinetic–spectral systems, where both wavelength and time ranges are chosen which are most adequate for the resolution of each mixture. The double information, kinetic and spectral, makes this selection complex, for which the development of simple procedures is advisable. Recently, the index of discrimination[10] has been proposed as a simple means of quantifying the kinetic–spectral discriminating effect of a multi-component system. It is evident that the smaller the coefficients of spectral and kinetic correlation between pairs of analytes, the greater is the difference between their signals and the easier their discrimination will be.

In this work, a simple method for the kinetic–spectral resolution of mixtures on the basis of the selection of the wavelength and time ranges that make their respective coefficients of correlation minimal is proposed. A set of simulated data for the kinetic reaction of two analytes giving two products and one interference with an overlapped spectra was generated in order to check the performance of the proposed method. Several rate constant ratios, producing different kinetic correlations, and several wavelength ranges for different degrees of overlap (interference–analytes) showing different spectral correlations were used. This method was applied to kinetic–spectrophotometric data obtained in the reaction of azo coupling of dyphylline and proxyphylline with the diazonium ion of sulfanilic acid, after alkaline hydrolysis (Fig. 1). Both dyphylline and proxyphylline are substances of pharmacological interest with bronchodilatory properties and have very similar structures, which suggests that their reaction rates and spectra will be very similar.

The chosen reaction was used for the determination of methylxanthines in medicines and has been described in the

DOI: 10.1039/b101201k

literature,[11–18] but in no case has it been used for the simultaneous kinetic–spectral resolution of dyphylline and proxyphylline.

Experimental

Simulations

Kinetic–spectrophotometric data for two analytes and a product that interferes in the determination were simulated using a program written using MATLAB v. 5.3 (The Math Works, Natick, MA, USA). The algorithm generates kinetic spectra by solving differential equations and assuming that only the reaction products absorb with Gaussian spectral bands. All the Gaussian bands were constructed with the same width (σ = 60 nm) and the same absorptivity coefficients every 1 nm over a wavelength range of 100 nm. The maximum of the band for the products of the analytes was kept constant at 23 and 27 nm, and the maximum for the interference was changed to be 40, 50, 60 and 70 nm. In all cases, adherence to Beer's law was presumed for each component and the total absorbance at each wavelength was assumed to be the sum of the absorbances of the components. The analyte concentrations were varied between 1.5×10^{-5} and 5.5×10^{-5} mol dm^{-3} and the interference concentration was kept constant at 1×10^{-5} mol dm^{-3}. Data were generated for nine standard calibration mixtures and for 12 unknown mixtures. In order to ensure pseudo-first-order kinetics in relation to the reagent, its concentration was 2.0×10^{-3} mol dm^{-3}. Under these conditions, 100 times were used in calculations, simulating that the observed fraction, as reaction, of the slower reacting species (interference) at the end of data collection was 99%. In order to study only the effect of spectral overlap and rate constant variations, the instrumental and rate constant noise contributions were kept constant at 1 and 5%, respectively. These values are based on previously published work.[19]

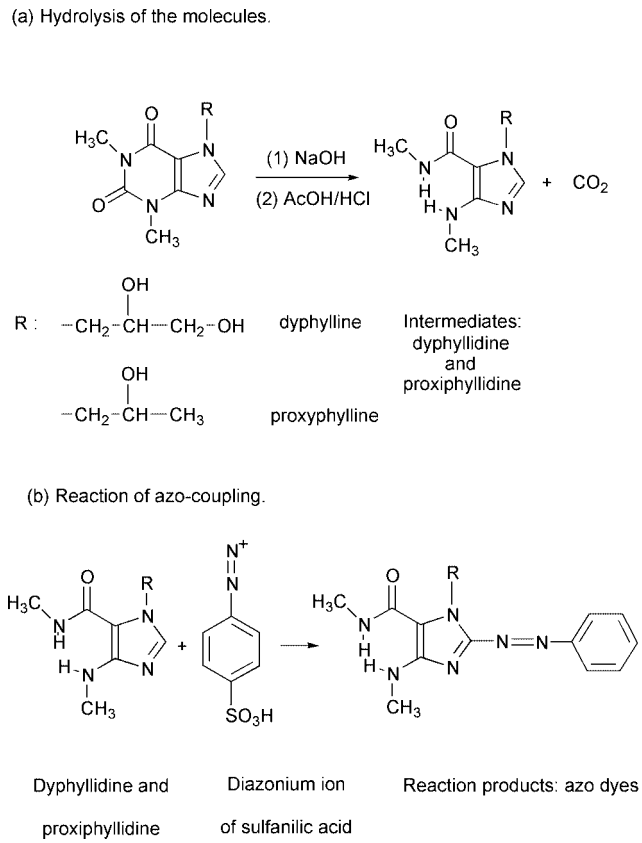

Fig. 1 Reactions of dyphylline and proxyphylline to form the azo coupling products.

A case without interference and four different relative positions of the interference and analytes, generating different spectral overlaps, were studied (Fig. 2). For each situation, four different wavelength ranges were used in the quantification: full spectrum and 30, 50 and 70 points. Finally, three rate constant ratios for the analytes (4, 2 and 1.2) were also considered. The total number of simulations was 60.

Apparatus

A Hewlett-Packard diode array spectrophotometer was used to acquire UV–Vis spectra at 2 nm intervals over the wavelength range 340–540 nm. Scans were performed at 1 s intervals (integration time 0.1 s) for 60 s using a thermostated cell of 1 cm pathlength at 25.0 ± 0.1 °C.

Reagents

All solutions were prepared in water obtained from a Milli-Q water purification system (Millipore). Stock standard solutions containing 7.56×10^{-2} mol dm^{-3} dyphylline [7-(2,3-dihydroxypropyl)theophylline] and proxyphylline [7-(2-hydroxypropyl)theophylline] (from Sigma) were prepared. Volumes of these solutions were mixed and diluted to 5 ml to obtain the working standard solutions.

Citric acid–NaOH buffer (pH 2.65) was prepared with a 0.5 mol dm^{-3} concentration with 1×10^{-3} mol dm^{-3} EDTA from stock standard solutions of citric acid monohydrate (Sigma, ACS reagent), NaOH (Carlo Erba, sodium hydroxide anhydrous pellets, ACS–ISO-f.a.) and EDTA (Panreac, ACS reagent f.a.). A 40% solution of NaOH was prepared as hydrolysis reagent.

A 3.6×10^{-2} mol dm^{-3} stock standard solution of diazonium ion of sulfanilic acid was prepared by mixing an apropriate amount of sulfanilic acid (Fluka, puriss. f.a.; ≥99.0%) with 1 cm^3 of concentrated HCl, 8 cm^3 of water and 4 cm^3 of 2% $NaNO_2$ (Aldrich ReagentPlus sodium nitrite, 99.99%). After cooling in an ice-bath for 15 min, 4 cm^3 of 2% sulfamic acid (PANREAC f.a.) were added to eliminate the excess of nitrite. Finally, the volume was completed to 25 ml with water.

Procedure

The working standard solutions of analytes were mixed with 5 cm^3 of 40% NaOH solution and heated for 1 h at 90 °C, then cooled to room temperature, neutralized with HCl–acetic acid to keep the pH between 5.5 and 6 and diluted to 100 cm^3 to obtain the final mixture. Volumes of 2.5 cm^3 of buffer, 0.1 cm^3 of final mixtures and 0.15 cm^3 of diazonium ion of sulfanilic acid were placed, with the aid of micropipettes, directly in the measuring cell. The system was kept at constant temperature with stirring throughout the reaction. The analyte concentrations in the measuring cell were in the range $(1.5–5.5) \times 10^{-5}$ mol dm^{-3} and were chosen based on the linear ranges obtained with single-analyte experiments. The calibration matrix was constructed following a 3^2 design and the predictive capacity of the different models tested was assessed by using a prediction set of 12 mixtures containing analyte concentrations within the calibration range. In order to include experimental variability factors, mixtures were prepared and measured in duplicate on different days.

Data processing

The UV–Vis spectra for each sample were recorded at p different wavelengths at k different times in order to construct three-way data arrays which were unfolded to obtain a classical two-dimensional data matrix in such a way that each row contained the spectrum for a mixture recorded at different times sequentially linked together ($\lambda_1 t_1$, $\lambda_2 t_1$, ..., $\lambda_p t_1$, ..., $\lambda_i t_j$, ..., $\lambda_1 t_k$, ..., $\lambda_2 t_k$, ..., $\lambda_p t_k$), so each column contained the absorbance measured at (λ_i ,t_j) for each sample. In order to achieve the best

predictive capacity, different spectral modes (absorbance and first derivative) and working wavelength ranges were tried. The derivative of the data matrix with respect to the wavelength at each time was obtained by using the Savitzky–Golay algorithm with a second-order polynomial and a window size of 11 points.

The data matrix thus obtained was centered and processed by using the PLS1 algorithm in the software Unscrambler v. 7.5 (CAMO, Trondheim, Norway). PLS1 models were constructed by cross-validation method and as many cross-validation segments as samples, each segment comprising the replicates of each sample. The optimum number of PLS1 components was determined in order to minimize the sum of the squared differences between known and determined concentrations:

$$\text{PRESS} = \sum_{i=1}^{n} (\hat{c}_i - c_i)^2 \quad (1)$$

where n is the number of samples, C_i is the known concentration and $\hat{C}_i$ is the determined concentration.

Two parameters were used to study the precision of the models: the standard error of prediction, SEP, and the standard deviation between replicates, SDBR. The SDBR parameter is calculated starting from the difference between the values obtained for replicates of the same composition, hence it is a measure of the experimental reproducibility, whereas SEP is calculated starting from the differences between the values found and those of reference, taking into account the bias of the values:

$$\text{SEP} = \sqrt{\frac{\sum_{1}^{n} (\hat{c}_i - c_i - \text{Bias})^2}{n-1}} \quad (2)$$

where the symbols have the same meaning as above, and the bias is:

$$\text{Bias} = \frac{\sum_{i=1}^{n} (\hat{c} - c_i)}{n} \quad (3)$$

The SDBR is defined by the expression:

$$\text{SDBR} = \sqrt{\frac{\sum_{1}^{k} (\hat{c}_{i,1} - c_{i,2})^2}{2k}} \quad (4)$$

where $C_{i,1}$ and $C_{i,2}$ are the determined concentrations of the replicates of each ith sample k is the number of different samples and the other symbols have the same meaning as above.

In the absence of any systematic effect, that is, when the model of calibration adjusts all of the samples well, SEP and SDBR should have similar values, which would indicate that the model of calibration is correct and that the differences found are due solely to experimental reproducibility. To test whether SEP does not vary significantly from the error between replicates, an F test ($\alpha = 0.05$) of significance of the corresponding variances was applied, F being calculated as:

$$F_{\text{calc}} = \frac{\text{SEP}^2}{\text{SDBR}^2} \quad (5)$$

where n is the degrees of freedom from the numerator and k those from the denominator.

Results and discussion

Simulations

One way of assessing the kinetic–spectrophotometric differences between two analytes is through the spectral and kinetic correlations,[10,20] which are defined mathematically as

$$\rho = \frac{\sigma_{12}}{\sigma_1 \sigma_2} \quad (6)$$

where σ_1 and σ_2 are the standard deviations of the spectral or kinetic profile for analytes 1 and 2 and σ_{12} is the spectral or kinetic covariance between the two.

For the calculation of the kinetic correlation coefficient, ρ_k, the variation of the signal with the time at the maximum of the band (absorbance or derivative) of each of the analytes is used,

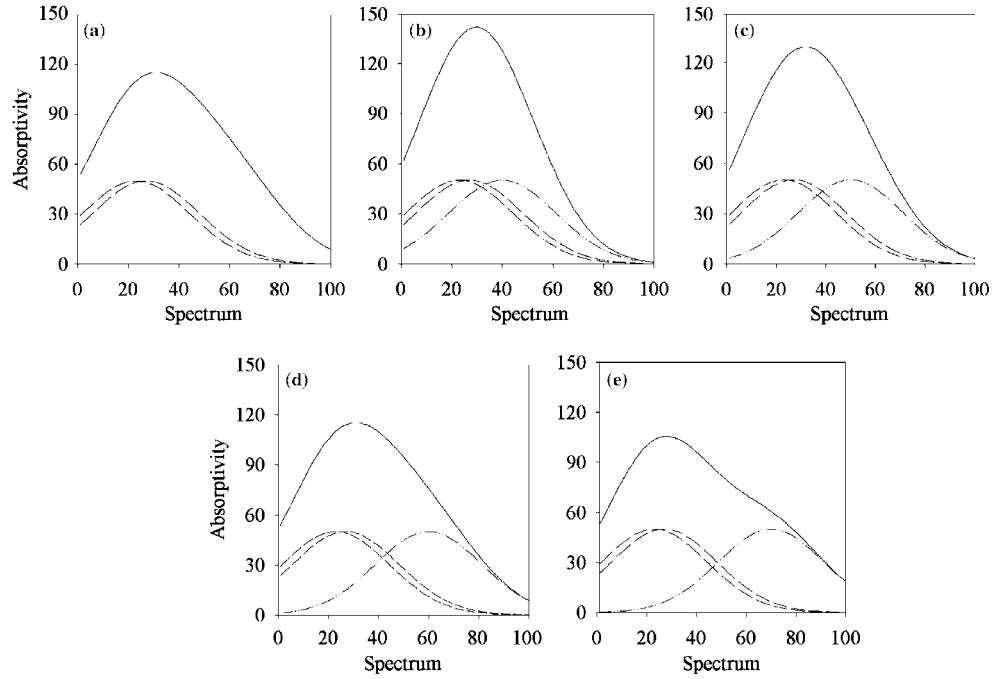

Fig. 2 Spectra of the three absorbing compounds used in the simulations. (– – –) Reaction products of the analytes; (– · · –) interference; (———) overall spectrum. (a) Without interference. Maximum of the interference at (b) 40, (c) 50, (d) 60 and (e) 70 nm.

whereas for the calculation of the spectral correlation coefficient, ρ_s, the spectrum of the reaction products of each of the analytes is used, in the mode considered (absorbance or derivative). A correlation coefficient close to unity means that the two analytes behave very similarly, so poor resolution is to be expected. On the other hand, a correlation coefficient close to zero reflects a great kinetic or spectral difference between analytes and the fact that the mixtures can be accurately resolved.

Fig. 3(a) shows the trend of ρ_k with the reaction time for the three rate constant ratios studied. As expected, the more similar the rate constants were, the higher were the kinetic correlations. A constant value of ρ_k is found when the reaction is completed. In Fig. 3(b), the variation of ρ_s with the wavelength range is plotted. Each curve represents a spectral overlap between the interference and the reaction products. As indicated, four different spectral ranges were used for the quantification of the analytes by means of a PLS1 regression.

The results obtained for both analytes in all the simulations as a function of the product ρ_k ρ_s are displayed in Fig. 4. This product could be understood as a simple measure of the overall kinetic–spectrophotometric difference between the two analytes. At low values, it is evident that sufficient information exists to resolve the system correctly, but beyond a certain value, around 0.98, there is not enough spectral and kinetic discrimination and PRESS increases considerably. This threshold should not be taken as an absolute value as it will depend on the noise level of the system studied.

Chemical system

The azo coupling reaction of the methylxanthines has been used previously in quantitative analysis using different coupling reagents.[11–18] Neither dyphylline nor proxyphylline reacts directly and a previous hydrolysis of the pyrimidine-like ring in an alkaline medium is necessary. Thus, the global process is divided into two stages as can be seen in Fig. 1. This process is influenced by factors such as the concentration of NaOH, the time for hydrolysis, the buffer, the pH, the reagent concentration and the preparation conditions. All of these factors were taken into account when designing the method and in the calibration process.

In the first stage, a study of NaOH concentration and the time of hydrolysis was made, the latter being one of the most determining factors for the analysis of the mixtures. The NaOH/analyte molar ratio was of the order of 500 : 1 and the optimum hydrolysis time was 60 min.

Prior to the process of azo coupling, neutralization was carried out owing to the elevated concentration of NaOH used in the first stage. This change of pH was accompanied by the release of CO_2 as is described in the literature for species of the same family.[21,22] The reactions of azo coupling take place very quickly at basic pH, and for this reason an acidic pH was chosen in order to permit spectrophotometric monitoring of the reaction. To carry out the pH study, citric acid–NaOH buffer was chosen. Between pH 2 and 4, the reaction rate of both species did not vary considerably, dyphylline always being the compound which showed a greater apparent reaction rate. pH 2.65 was used for performing the calibration. A concentration of the diazonium ion of sulfanilic acid of 2×10^{-3} mol dm^{-3} was chosen in the measuring cell with sufficient excess so that the kinetics were of pseudo-first order with respect to the analytes.

Fig. 5 shows the kinetic–spectrophotometric spectra for the reaction of 2×10^{-3} mol dm^{-3} diazonium ion of sulfanilic acid with a mixture of 3.5×10^{-5} mol dm^{-3} dyphylline and proxyphylline at pH 2.65 and 25 °C. There is a band between 340 and 390 nm which increases over time and another between 390 and 440 nm which initially increases quickly but after 3 s begins to decrease. Under these experimental conditions, both dyphylline and proxyphylline exhibit a reaction time of about 60 s. As can be seen in Fig. 6, both the absorbance and the derivative spectra for the reaction products are very similar. Thus, both the kinetic and spectral information was necessary to allow the analysis of mixtures.

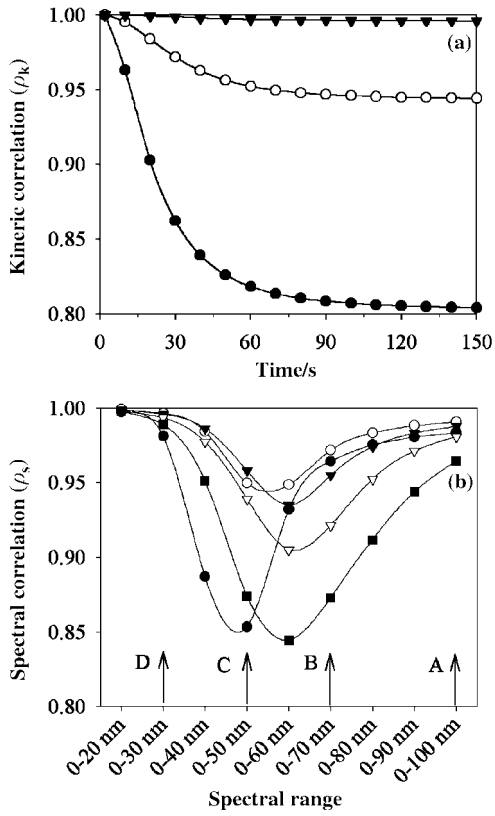

Fig. 3 (a) Variation of the kinetic correlation coefficient with time for different rate constant ratios: (●) k_1/k_2 = 4; (○) k_1/k_2 = 2; (▼) k_1/k_2 = 1.2 (b) Variation of the spectral correlation with the wavelength range; (●) no interference; (○) interference at 40 nm; (▼) interference at 50 nm; (▽) interference at 60 nm; (■) interference at 70 nm. Arrows A, B, C and D indicate the wavelength ranges assayed in the quantification of the analytes.

Determination of dyphylline and proxyphylline mixtures

The correlation coefficients can be used for selecting the range of wavelengths and the total recording time which provide the greatest discrimination between dyphylline and proxyphylline. The first-derivative spectrum was used in this work to carry out

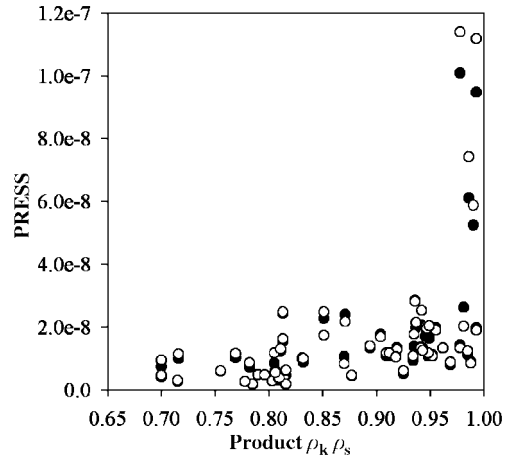

Fig. 4 Variation of PRESS with the product $\rho_k\rho_s$. (●) Fast analyte; (○) slow analyte.

the study of the ranges of wavelengths and time since it corrects the deviation of the baseline and increases the spectral resolution.

From the first-derivative spectrum in Fig. 6(b) for both species, a wavelength of 378 nm was chosen for calculating the kinetic correlation at different time intervals. In Fig. 7(a), it can be seen how the correlation diminishes with increase in recording time up to 60 s, after which point the correlation begins to slightly increase. Hence, this time was chosen as optimum for the recording of the mixtures and for the PLS1 calculations.

A greater difficulty was experienced in the selection of the range of wavelengths since the kinetics of the system showed two apparently important bands for the correct resolution. The starting point was from the derivative spectrum to infinite time [Fig. 6(b)] for each of the analytes, so the kinetic correlation coefficient was fixed and the spectral correlation coefficient for different ranges of wavelengths was calculated. As can be seen, the correlation diminishes as the interval shortens to a minimum, 350–410 nm, from which point it begins to increase again up to almost unity.

SEP and SDBR for the external prediction set are compared in Table 1 for different intervals of wavelengths using a 60 s recording time and it is observed that the best results were obtained in the wavelength interval 350–410 nm, which presented less spectral correlation [Fig. 7(b)] and the minimum value of the product $\rho_k\rho_s$. It is also observed that as the wavelength interval diminishes, the number of variables used in the calculation is reduced, so the models obtained are easier to interpret (Table 1). In cases the results obtained for proxyphylline are better than those for dyphylline, possibly owing to its greater molar absorptivity. A simpler interpretation of the quality of the results can be made by calculating the values of SEP and SDBR relative to the average concentration, these being of the order of 4 and 3% for dyphylline and proxyphylline, respectively. For all of the models, applying the *F* test of significance, the standard errors of prediction in terms of error do not differ significantly from the difference between replicates, hence PLS1 correctly quantifies both analytes. Nevertheless, it is observed that as the selected interval of wavelengths diminishes, the SEP and SDBR values diminish, thus increasing the precision of the models. Table 2 gives the individual results obtained with PLS1 using the wavelength range 350–410 nm for the prediction set. The regression parameters for the prediction of dyphylline are intercept = $(0.46 \pm 1.88) \times 10^{-6}$ mol dm^{-3}, slope = 0.958 ± 0.051, r = 0.992, and for proxyphylline intercept = $(0.16 \pm 1.75) \times 10^{-6}$ mol dm^{-6}, slope = 0.981 ± 0.048, r = 0.993.

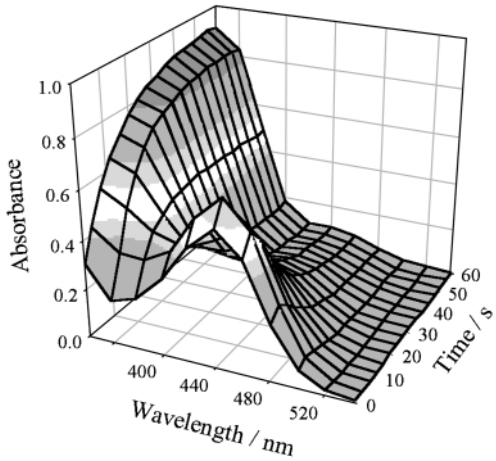

Fig. 5 Kinetic–spectrophotometric spectra for the reaction of a mixture of 3.5×10^{-5} mol dm^{-3} dyphylline and 3.5×10^{-5} mol dm^{-3} proxyphylline with 2×10^{-3} mol dm^{-3} diazonium ion of sulfanilic acid Citric acid–NaOH–EDTA buffer at pH 2.65 and 25 °C. Spectra were recorded from 0 to 60 s at 1 s intervals over the wavelength range 340–540 nm.

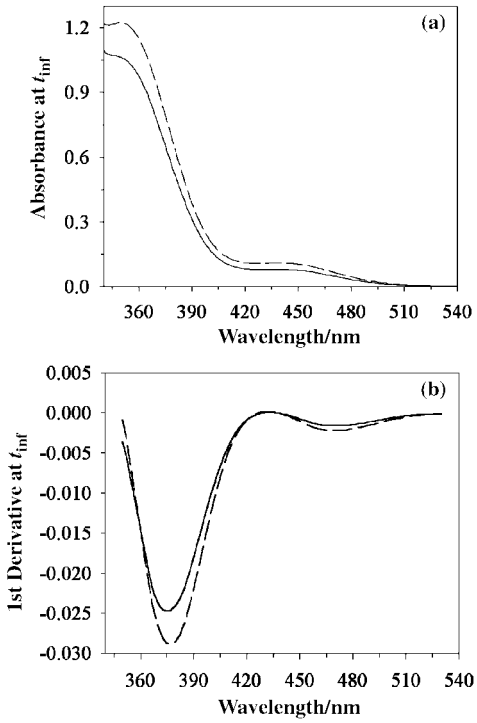

Fig. 6 (a) UV–Vis spectra and (b) first-derivative spectra of the reaction products of dyphylline (——), and proxyphylline (– – –), both at 1×10^{-4} mol dm^{-3} concentration with 2×10^{-3} mol dm^{-3} diazonium ion of sulfanilic acid. Citric acid–NaOH–EDTA buffer at pH 2.65 and 25 °C.

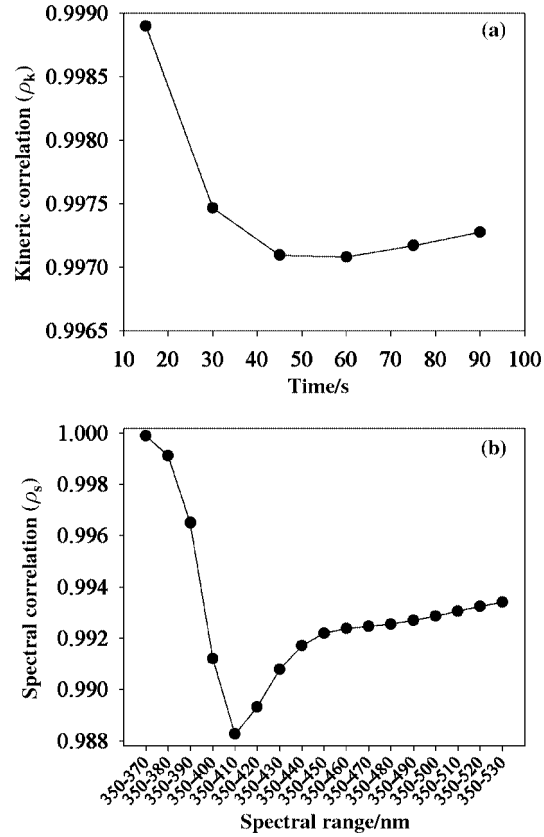

Fig. 7 (a) Variation of the kinetic correlation coefficient (ρ_k) between dyphylline and proxyphylline with the time range. (b) Variation of the spectral correlation coefficient (ρ_s) between the reaction products of dyphylline and proxyphylline with the wavelength range. [Analyte] = 1×10^{-4} mol dm^{-3}; [diazonium ion] = 2×10^{-3} mol dm^{-3}; citric acid–NaOH–EDTA buffer at pH 2.65 and 25 °C.

Table 1 SEP [eqn. (2)] and SDBR [eqn. (4)] obtained in the determination of dyphylline and proxyphylline in the prediction set using PLS1 models and different spectral ranges

Wavelength range/nm	Variable/ sample	$\rho_k\rho_s$	Dyphylline[a]		Proxyphylline[a]	
			SEP	SDBR	SEP	SDBR
350–530	5460	0.9910	2.15×10^{-6}	1.86×10^{-6}	1.69×10^{-6}	1.62×10^{-6}
350–470	3660	0.9896	1.95×10^{-6}	1.62×10^{-6}	1.49×10^{-6}	1.38×10^{-6}
350–410	1860	0.9854	1.50×10^{-6}	0.97×10^{-6}	1.18×10^{-6}	0.77×10^{-6}

[a] Number of PLS components used in the models = 3.

Table 2 Results obtained in the resolution of mixtures of dyphylline and proxyphylline in the prediction set using PLS1 and the wavelength range 350–410 nm

Sample	Dyphylline[a]			Proxyphylline[a]		
	Added $\times 10^5$/ mol dm^{-3}	Found $\times$ 10^5 / mol dm^{-3}	Absolute error $\times$ 10^5 /mol dm^{-3}	Added $\times$ 10^5/ mol dm^{-3}	Found $\times$ 10^5/ mol dm^{-3}	Absolute error $\times$ 10^5/mol dm^{-3}
M1a	2.29	2.23	-0.05	2.28	2.24	−0.04
M1b	2.29	2.21	−0.07	2.28	2.25	−0.03
M1c	2.30	2.27	−0.03	2.30	2.33	0.03
M1d	2.30	2.34	0.04	2.30	2.28	−0.02
M2a	5.29	5.33	0.04	2.28	2.16	−0.12
M2b	5.29	4.98	−0.31	2.28	2.45	0.17
M2c	5.32	5.34	0.02	2.30	2.38	0.08
M3a	3.91	3.95	0.04	2.75	2.68	−0.07
M3b	3.91	4.08	0.17	2.75	2.59	−0.17
M4a	2.97	2.82	−0.15	3.22	3.17	−0.05
M4b	2.97	2.88	−0.09	3.22	3.17	−0.05
M5a	1.85	1.94	0.09	3.44	3.49	0.05
M5b	1.85	1.86	0.01	3.44	3.53	0.09
M6a	4.60	4.51	−0.09	3.44	3.32	−0.12
M6b	4.60	4.47	−0.13	3.44	3.32	−0.12
M7a	3.44	3.28	−0.16	3.66	3.69	0.03
M7b	3.44	3.44	0.00	3.66	3.58	−0.08
M8a	2.29	2.14	−0.15	3.90	3.85	−0.05
M8b	2.29	2.09	−0.20	3.90	3.86	−0.04
M9a	4.85	4.59	−0.26	3.93	3.65	−0.28
M9b	4.85	4.77	−0.08	3.93	3.62	−0.31
M10a	3.66	3.46	−0.20	4.59	4.50	−0.09
M10b	3.66	3.53	−0.13	4.59	4.34	−0.25
M11a	2.75	2.76	0.01	5.03	4.91	−0.12
M11b	2.75	2.62	−0.13	5.03	4.97	−0.06
M12a	4.60	4.11	−0.49	5.28	5.43	0.15
M12b	4.60	4.17	−0.43	5.28	5.33	0.05

[a] Number of PLS components used in the models = 3.

Conclusions

A rapid, simple and easily interpreted method for the selection of variables in kinetic–spectrophotometric systems which does not require the use of complicated calculation methods and specific software has been developed. The reduction in the number of variables permits the construction of more rapid models that are easy to interpret, and provides better results since it eliminates the least important information related to the system under study.

Once again it is evident that the PLS1 multivariable calibration technique is a powerful mathematical tool for the kinetic–spectrophotometric resolution of mixtures of analytes which show great spectral overlap and similarity in kinetic behavior as opposed to a common reagent.

Acknowledgements

The authors are grateful to the DGICyT, Spain, for funding this research within the framework of Projects PB97-0213 and PB96-1180. M. Porcel acknowledges additional support from the Spanish Ministry of Science and Technology in the form of an FPI grant.

References

1 H. Marterns and T. Naes, *Multivariate Calibration*, Wiley, New York, 1989.
2 S. R. Crouch, A. Scheeline and E. S. Kirkor, *Anal. Chem.*, 2000, **72**, 53R.
3 T. F. Cullen and S. R. Crouch, *Mickrochim. Acta*, 1997, **126**, 1.
4 S. D. Frans and J. M. Harris, *Anal. Chem.*, 1985, **57**, 2680.
5 A. S. Barros and D. N. Rutledge, *Chemom. Intell. Lab. Syst.*, 1998, **40**, 65.
6 R. Leardi and A. L. González, *Chemom. Intell. Lab. Syst.*, 1998, **41**, 195.
7 A. Herrero and M. C. Ortiz, *Anal. Chim. Acta*, 1999, **378**, 245.
8 L. G. Weyer and S. D. Brown, *J. NIR*, 1996, **4**, 163.
9 M. Azubel, F. M. Fernández, M. B. Tudino and O. E. Troccoli, *Anal. Chim. Acta*, 1999, **398**, 93.
10 S. R. Crouch, J. Coello, S. Maspoch and M. Porcel, *Anal. Chim. Acta*, 2000, **424**, 115.
11 P. Depovere, M. Piraux and T. Adzet, *Circ. Farm.*, 1975, **33**, 623.
12 J. C. Chiarino, *An. Asoc. Quim. Farm. Urug.*, 1951, **51**, 13.
13 H. Raber, *Sci. Pharm.*, 1964, **32**, 122.

14 R. Ott and H. Wittmann-Zinke, *Sci. Pharm.*, 1958, **26**, 217.
15 M. Mariani-Scotti, *Boll. Chim. Farm.*, 1965, **104**, 356.
16 S. R. El-Shabouri, S. A. Hussein and S. E. Emara, *Talanta*, 1989, **36**, 1288.
17 G. Fleischer, *Pharmazie*, 1956, **11**, 208.
18 M. P. de Castro and R. Rey, *Inf. Quím. Anal.*, 1963, **17**, 158.
19 M. Blanco, J. Coello, H. Iturriaga, S. Maspoch, M. Redón and J. F. Rodríguez, *Quím. Anal.*, 1996, **15**, 266
20 T. F. Cullen and S. R. Crouch, *Anal. Chim. Acta*, 2000, **407**, 35.
21 R. Pohloudek-Fabini, G. Döge and D. Kottke, *Pharmazie*, 1984, **39**, 24.
22 G. Peinhardt, *Pharmazie*, 1991, **46**, 812.

KINETIC SPECTROPHOTOMETRIC DETERMINATION OF THEOPHYLLINE, DYPHYLLINE AND PROXYPHYLLINE IN A PHARMACEUTICAL PREPARATION BY USE OF PARTIAL LEAST SQUARES REGRESSION.

ABSTRACT

A kinetic-spectrophotometric method for the determination of theophylline, dyphylline and proxyphylline, based on its azo coupling reaction with the diazonium ion of sulfanilic acid after a treatment with alkali is proposed. The absorbance is recorded from 340 to 600 nm, each second during 90 seconds of reaction, and calibration is performed by partial least-squares regression, using first derivative spectra values. Mixtures containing 2.5-13 ppm of dyphylline and proxyphylline, and 2-9 ppm of theophylline were successfully resolved with root mean squared errors of prediction (RMSEP) of 0.4, 0.3 and 0.2 for dyphylline, proxyphylline and theophylline, respectively. The proposed method was satisfactorily applied to the determination of the three compounds in a commercially available pharmaceutical preparation and provided similar results than those obtained by HPLC procedure.

1.INTRODUCTION

Kinetic methods of analysis present certain potential advantages with respect to methods based on equilibrium and are based on the resolution of systems on the basis of the different reaction rate of their components with a common reagent. Their advance in recent years[1] means that, more and more, they are taken into account for the resolution of mixtures of very similar species. Normally, the reaction can be monitored by means of the spectrophotometric register of the signal related to the reaction products or the disappearance of the signal of the reacting species. Particularly interesting for these applications are the UV-Vis spectrophotometric diode-array detectors which allow signal register at many different wavelengths in a short time, hence they have been used in kinetic systems.

The development of multivariable calculation software has made possible the treatment of the great quantity of kinetic-spectral information obtained.[2] Thus, a large number of mathematical methods are available, curve fitting,[3] non-linear regression[4,5] and the Kalman filter[6-8] have been used for this purpose. The main drawback of all these methods is that some parameters of the system, for example the kinetic model, must be known in advance. This is not the case of other multivariate calibration methods[9] such as PLS, PCR, and ANN. These methods provide advantages such as the resolution of mixtures without prior knowledge of the kinetic model followed by the system, rate constants, absorptivities, etc.; the ability to process complex kinetic systems[10-15] (interactions between analytes, the effects of slight interferences from species reacting with a general reagent or perturbations in the data matrix) and the resolution of mixtures of absorbent species that overlap strongly.[2,16,17] On the other hand, some of them can be applied not only to linear but also to non-linear systems.[9,18-20]

Recently, the ability of the PLS methods has been successfully employed in the simultaneous resolution of binary,[21,22] ternary,[23,24] quaternary[25] and quinquenary[26] mixtures.

In this work, a kinetic-spectrophotometric method has been developed for the simultaneous determination of dyphylline, proxyphylline and theophylline based on the reaction of these methylxantines with the diazonium ion of sulfanilic acid. The azo coupling reaction of methylxantines is widely documented and applied for analytical purposes.[27-32] Theophylline possesses an active hydrogen in position 8 (Fig.1) and can azocopulate with a salt of

diazonium due to this position having a certain nucleophile character. This property has been used as an identification system of theophylline in the presence of other species with a great variety of copulating agents[27]. The nucleophile character is not so evident in dyphylline and proxyphylline and an esteric hindrance exists associated to the functional group situated in 7-N which makes a previous pre-treatment in alkaline medium necessary in order to increase the nucleophile character and to achieve the azo coupling. This pre-treatment consists of alkaline hydrolysis with the consequent destruction of the pyrimidinic nucleus. This same treatment had already been described for theophylline and other species of the same family, such as caffeine.[27,28] The process of hydrolysis is followed by a neutralization with the consequent detaching of CO_2 such as is described in the bibliography for substances of the same family.[33,34] In the azocopulation process, reaction products are obtained which absorb in the visible region and which can be used for the identification of this family of species.

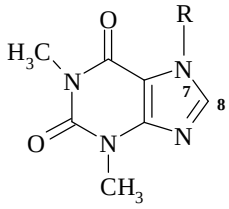

R : -H theophylline

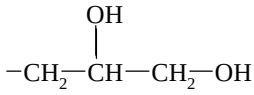

dyphylline

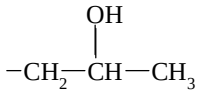

proxyphylline

Figura 1. Structures of the compounds

Thus, the specific purpose was to analyse the active compounds in the commercially available preparation Novofilin Retard, which contains them as active compounds. This pharmaceutical is principally used in the prevention and treatment of bronchial asthma due to the bronchio-dilatory properties of its three active components. Despite the high chemical similarity between the dyphylline and proxyphylline (see Fig. 1), a previous work[35] shows that their

simultaneous kinetic determination using PLS1 is possible. Calibration was performed by using PLS1 regression and the results were compared with those provided by high performance liquid chromatography (HPLC) as an alternative validation method.[36] The proposed kinetic-spectrophotometric method avoids the step of extraction of the compounds from the insoluble components of the tablets required by the HPLC procedure. Theophylline has a low solubility in water, while dyphylline and proxyphylline do not present problems of solubility.

2. EXPERIMENTAL

Apparatus.

A Hewlett-Packard diode array spectrophotometer, HP-8453A, was used to acquire UV-Vis spectra at 2 nm intervals over the wavelength range 340-600 nm. Scans were performed at 1 s intervals (integration time 0.1 s) for 90 seconds using a thermostated cell of 1 cm pathlength at 25.0 ± 0.1ºC.

The chromatographic determination was carried out by using a system consisting of Shimadzu (Kyoto, Japan) LC-10AD pumps, a Hewlett-Packard 1040A HPLC diode array UV-Vis spectrophotometer and a Model 9153C data station, also from Hewlett-Packard. A Spherisorb ODS-2C_{18} column (15 cm long x 0.46 cm id, 5 μm particle size, Tracer) was employed.

Reagents.

All solutions were prepared in water from a Mili-Q water purification system (Millipore). Stock standard solutions containing a $7x10^{-2}$ mol dm^{-3} dyphylline [7-(2,3-dihydroxypropyl)theophylline], proxyphylline [7-(2-hydroxypropyl)theophylline] and theophylline (from Sigma) were prepared. Volumes of these solutions were mixed and diluted to 5 ml to obtain the working standard solutions.

Citric acid-NaOH buffer (pH 2.65) was prepared with 0.5 mol dm^{-3} concentration with $1x10^{-3}$ mol dm^{-3} of EDTA from stock solutions of citric acid monohydrate (Sigma, ACS Reagent), NaOH (Carlo Erba, sodium hydroxide anhydrous pellets, ACS-ISO-p.a.) and EDTA (Panreac,

ACS reagent p. a.).

A 40% solution of NaOH was prepared as hydrolysis reagent.

A 3.6 x 10^{-2} mol dm^{-3} stock standard solution of diazonium ion of sulfanilic acid was prepared by mixing an appropriate amount of sulfanilic acid (Fluka puriss. p.a.; ≥ 99.0%) with 1 cm^3 of HCl concentrated, 8 cm^3 of water and 4 cm^3 of 2 % $NaNO_2$ (Aldrich ReagentPlus, sodium nitrite, 99.99%). After cooling in an ice-bath for 15 min, 4 cm^3 of 2% sulfamic acid (Panreac p.a.) were added to eliminate the excess nitrite. Finally, the volume was completed up to 25 cm^3 with water.

Real samples.

The samples studied belonged to one production batch of the pharmaceutical preparation Novofilin Retard (from Ferrer International, S. A., Barcelona, Spain) and were purchased at a chemist. The preparation is available as a box of 40 tablets and the stated concentrations were 75.0 mg of theophylline, 112.5 mg of dyphylline and 112.5 mg of proxyphylline per tablet as active compounds.

Kinetic-spectrophotometric procedure.

Calibration mixtures.

The working standard solutions of analytes were mixed with 5 cm^3 of 40% NaOH solution and heated during 1 h at 90ºC, then cooled to room temperature, neutralized with HCl / acetic acid to keep the pH between 5.5 and 6 and diluted to 100 cm^3 to obtain the final mixtures.

Volumes of 2.5 cm^3 of buffer, 0.1 cm^3 of final mixtures and 0.15 cm^3 of diazonium ion of sulfanilic acid were added, with the aid of micropipettes, directly in the measuring cell. The system was kept at constant temperature with stirring throughout the reaction. The analyte concentrations in the measuring cell were in the range 2.5-13 ppm for dyphylline and proxyphylline, 2-9 ppm for theophylline; and were chosen based on the linear ranges obtained with single-analyte experiments. The calibration matrix was constructed following a 3^3 design with replicates for each point and the predictive capacity of the different models tested was assessed by using a prediction set of 14 mixtures (random selection between the range

concentrations), which contained analyte concentrations within the calibration range. In order to include experimental variability factors, mixtures were prepared and measured in duplicate on different days.

Real sample.

Novofilin Retard samples were prepared by weighing and milling 20 tablets. From the milled, five portions of about 0.1 g were mixed with 10 ml of water and 10 ml of 40 % NaOH solution, heated and processed in the same way as the laboratory mixtures prepared. Three or four kinetic-spectrophotometric replicates were recorded from each amount weighed. Before recording the kinetic reaction, the solutions were filtered in order to remove the insoluble compounds of the tablets. The concentrations in the measuring cell correspond to the center of the calibration model.

Chromatographic procedure.

Prior to chromatographic analysis, the active compounds must be removed from the tablets. To this end, three portions of about 0.1 g of the pharmaceutical milled were weighed and placed in a centrifuge tube with 100 ml of water. It was immersed in an ultrasonic bath for enough time to ensure the extraction of the soluble products and then centrifuged and filtered. A portion of 10 ml of each filtered was diluted to 100 ml to obtain the final solution. A 20 μl portion of these final solutions was passed through a nylon filter of 0.45 μm pore size and eluted with an acetic buffer-acetonitrile-methanol (91:4:5) mobile phase at a constant flow-rate of 1.5 ml min^{-1}. The concentration range where the integrated peak area was linearly related to the concentration was examined and calibration curves were run from solutions containing variable concentrations of each active compound. The central concentration was very close to the theoretical concentration in the pharmaceutical.

Under these conditions, well-defined, well-resolved, tailless peaks were obtained with retention times 10.0 ± 0.1, 11.8 ± 0.1 and 27.7 ± 0.2 minutes for theophylline, proxyphylline and dyphylline, respectively. Samples were injected in triplicate and their chromatograms recorded at the maximum absorption wavelength of 274 nm using a bandwidth of 4 nm.

Data acquisition and processing

The UV-Vis spectra for each sample were recorded at *p* different wavelengths at *k* different times in order to construct three-way data arrays which were unfolded to obtain a classical two-dimensional data matrix in such a way that each row contained the spectrum for a mixture recorded at different times sequentially linked together *(l_1t_1, l_2t_1,..., l_pt_1,..., l_it_j,..., l_1t_k,..,. l_2t_k,..., l_pt_k)*, so each column contained the absorbance measured at (λ_i, t_j) for each sample. Data matrix **Y** contained the concentrations of dyphylline, proxyphylline and theophylline. In order to achieve the best predictive capacity, different spectral modes (absorbance and derivative) and working wavelength ranges were tried. The derivative of the data matrix with respect to the wavelength at each time was obtained by using the Savitzky-Golay algorithm with a second-order polynomial and a window size of 11 points.

The data matrix **X** thus obtained was centered and then processed by using the PLS1 algorithm in the software Unscrambler v. 7.5 (CAMO, Trondheim, Norway). PLS1 models were constructed by cross-validation, using as many cross-validation segments as samples, each segment comprising the replicates of each sample. The optimum number of PLS1 components was determined in order to minimize the sum of the squared differences between known and determined concentrations,

$$\mathrm{PRESS} = \sum_{i=1}^{n} \left(c_i - \hat{c}_i\right)^2 \qquad (1)$$

where *n* is the number of samples, C_i is the known concentration and $_i$ the determined concentration.

The results obtained in the quantification of the samples in the calibration and prediction set are expressed as root mean square errors of calibration (RMSEC) and of prediction (RMSEP), respectively. The last is given by

$$RMSEP = \sqrt{\frac{PRESS}{m}} \qquad (2)$$

where *m* is the number of samples in the prediction set.

3. RESULTS AND DISCUSSION.

Kinetic-spectrophotometric resolution of mixtures.

Chemical System.

The global process is influenced by factors such as NaOH concentration, hydrolysis time, the buffer, pH and the reagent concentration as well as its conditions of preparation. Thus, all of these factors have been taken into account when designing the method and in the calibration process.[35]

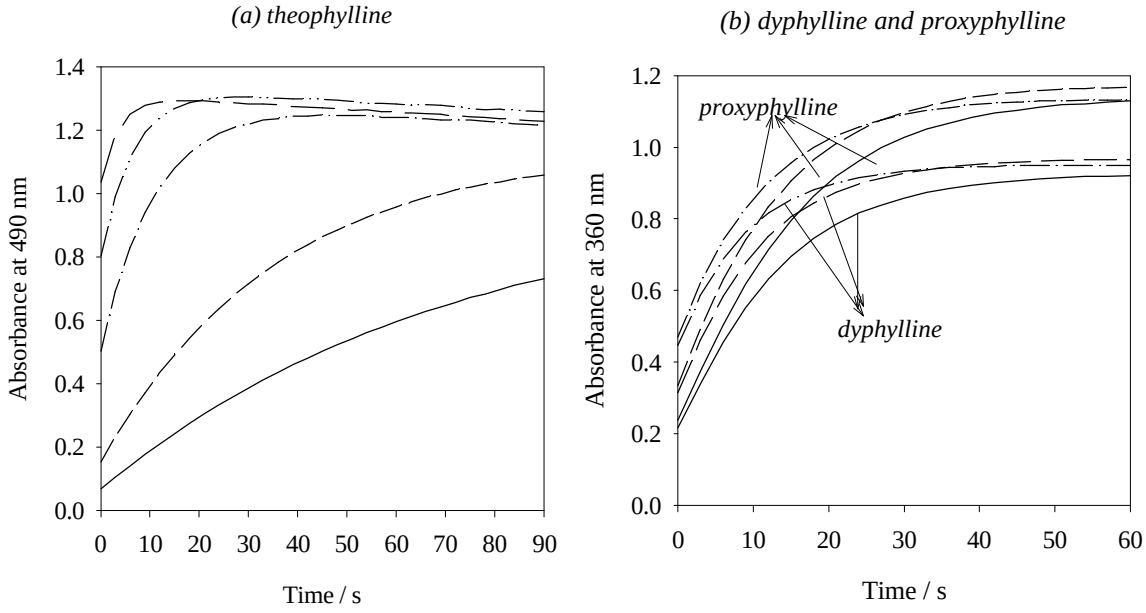

Figura 2. (a) Variation of the kinetic profile, at 490 nm, with the pH for $5x10^{-5}$ mol dm^{-3} theophylline, (—) pH 2.39; (- - -) pH 2.58; (- · -) pH 3.04; (- · · -) pH 3.30; (– –) pH 3.59. (b) Variation of the kinetic profile with the pH for $1x10^{-4}$ mol l^{-1} dyphylline and proxyphylline, (–) pH 2.39; (- - -) pH 2.58; (- · -) pH 3.04. [diazonium ion]=$2x10^{-3}$ mol dm^{-3}; citric ac.-NaOH-EDTA buffer and T=25ºC.

In order to monitor the azo coupling reaction, an acid pH was used since in a basic medium the reaction takes place very quickly. The buffer used was the citric acid-NaOH one and the study was performed between pH 2 and 4. Dyphylline and proxyphylline are not very influenced by the pH changes but theophylline considerably modifies its reaction rate as well as the spectrum of the reaction product moving the maximum of absorption towards superior wavelengths to higher pHs. As is seen in Fig. 2(a), the apparent rate of theophylline

considerably increases with the pH to the point that spectrophotometric monitoring of the reaction is not possible with the mixing and detection systems used. In Fig. 2(b) the kinetic profiles at 360 nm of dyphylline and proxyphylline at three very close pHs: 2.39, 2.58 and 3.04 are shown. It is observed that the apparent reaction rate of dyphylline and proxyphylline is very similar, proxyphylline showing more absorptivity. For the three species, as the pH increases it becomes more difficult to perform the register of initial times of reaction. In order to perform the calibration, a buffer at pH 2.65 was chosen. At this pH the reaction is completed in 90 s for theophylline, and in 60 s for dyphylline and proxyphylline.

A concentration, in the measuring cell, of $2x10^{-3}$ mol dm^{-3} of diazonium ion of sulfanilic acid was chosen, which was sufficient for the kinetics to be of pseudo-first order, with respect to the analytes.

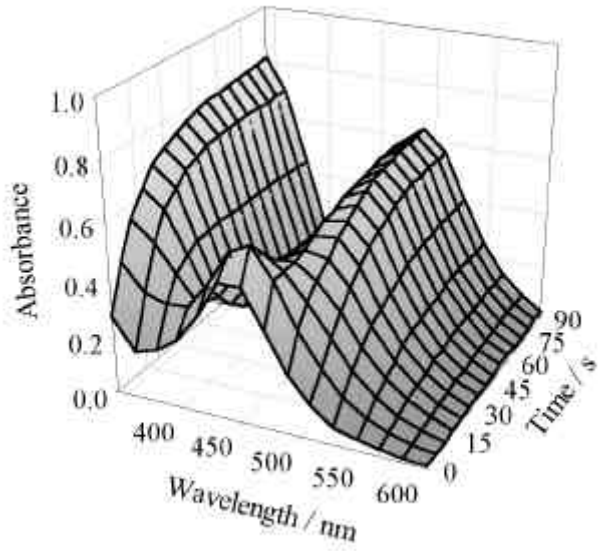

Figura 3. Kinetic-spectrophotometric spectra for the reaction of a mixture of 7.7 ppm dyphylline, 7.2 ppm proxyphylline and 5.4 ppm theophylline with $2x10^{-3}$ mol dm^{-3} diazonium ion of sulfanilic acid. Citric ac.-NaOH-EDTA buffer at pH 2.65 and 25ºC. Spectra were recorded from 0 to 90 s at 1s intervals over the wavelength range 340-600 nm.

Fig. 3 shows the kinetic-spectrophotometric spectra for the reaction of $2x10^{-3}$ mol dm^{-3} of diazonium ion of sulfanilic acid with a mixture of 7.7 ppm dyphylline, 7.2 ppm proxyphylline and 5.4 ppm theophylline at pH 2.65 and 25ºC. As can be seen, there is a band between 340-

390 nm that increases over time and another between 390-440 nm that initially increases quickly and after 3 seconds begins to decrease. These two bands are due to dyphylline and proxyphylline. Another band, increasing over the time at 490 nm, is due to the theophylline. This band is affected by the pH, so this must be carefully controlled. As can be seen in Fig. 4, both the absorbance and the derivative spectra for the reaction products are very similar for dyphylline and proxyphylline, being very different from theophylline.

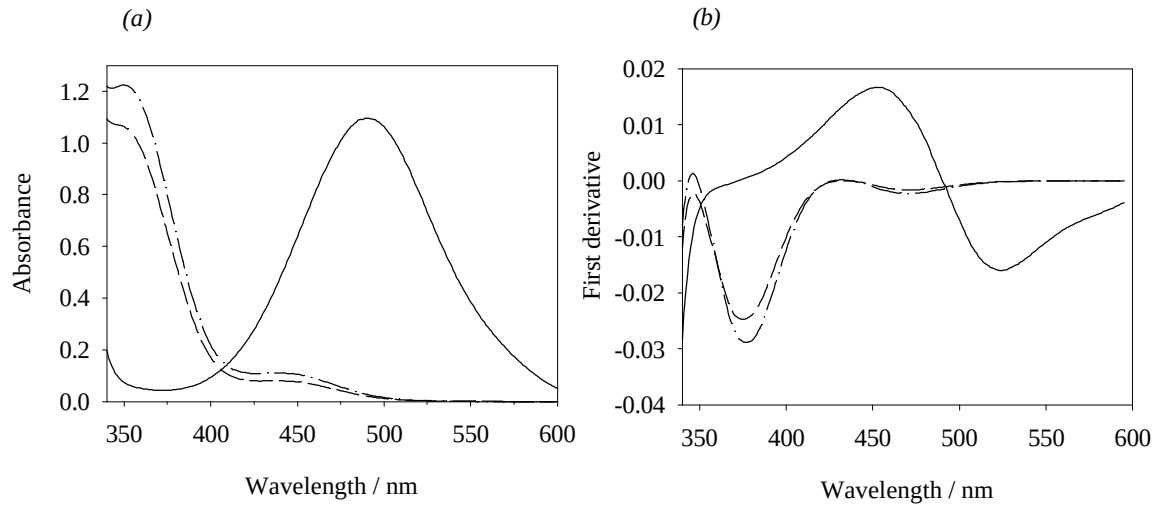

Figura 4. (a) UV-Vis spectra and (b) first derivative spectra of the reaction products of dyphylline (– –), proxyphylline (- · -) both at $1x10^{-4}$ mol dm^{-3} concentration and $5x10^{-5}$ mol dm^{-3} theophylline (—) with $2x10^{-3}$ mol dm^{-3} diazonium ion of sulfanilic acid. Citric ac.-NaOH-EDTA buffer at pH 2.65 and 25ºC.

PLS calibration.

PLS calibration allows one to use all the kinetic-spectrophotometric information. The compounds of the tablets not eliminated by filtration could produce scattering of the light and change the solution absorbance by a wavelength-independent factor. This effect can be corrected by using derivatives of the original spectra rather than direct absorbance measurements. Although PLS can process high data matrix it may be useful to exclude the variables contributing with no analytically significant information. The selection was made by choosing various wavelength ranges and times. No significant differences between models were obtained at different time intervals, so the total registered time was used. The first

recorded spectrum was suppressed in the calculations to insure that the data had been registered in homogeneous conditions in the measuring cell. The results of the quantification for different wavelengths ranges studied are shown in Table 1. It is seen that all of the information registered is not necessary for the correct quantification of the mixtures. For the three analytes, the band situated between 410-470 nm can be omitted because it does not contribute analytical information to the system and the fact of using it only implies the use of more PLS components. For theophylline the same results were obtained for all of the wavelength ranges tested, and for dyphylline as well as for proxyphylline it was necessary to take into account the absorbance band of theophylline of 470-550 nm for a correct quantification.

Table 1. RMSEC and RMSEP obtained at different wavelength ranges using PLS1 and 1st derivative mode for laboratory prepared samples.

Wavelength range	**Dyphylline**		**Proxyphylline**		**Theophylline**	
	RMSEC	RMSEP	RMSEC	RMSEP	RMSEC	RMSEP
350-590 nm[a]	0.35	0.40	0.24	0.31	0.20	0.13
350-410; 470-550 nm[b]	**0.39**	**0.43**	**0.25**	**0.31**	**0.20**	**0.13**
350-410 nm[c]	0.45	0.62	0.31	0.32	-	-
470-550 nm[d]	-	-	-	-	0.20	0.13

Number of PLS components used in the models: a) 7 for dyphylline and proxyphylline; and 2 for theophylline. b) 6 for dyphylline and proxyphylline; and 2 for theophylline. c) 6 for dyphylline and proxyphylline. d) 1 for the theophylline.

Determination of theophylline, dyphylline and proxyphylline in Novofilin Retard.

Once the proposed method was checked to provide such a good results with samples prepared in the laboratory, it was applied to the analysis of the pharmaceutical preparation, Novofilin Retard. The best PLS1 results for each analyte have been those obtained with the wavelength ranges 350-410 and 470-550 nm, and are compared in Table 2 with those provided by the HPLC (average values and their corresponding confidence intervals at α=0.05). As can be seen, there are not significant differences between the values obtained with the kinetic-spectrophotometric and the HPLC methods. For the specific case of dyphylline, the kinetic

method provides a greater dispersion in the results, which can be due to the lower absorptivity of this specie.

Table 2. Average theophylline, dyphylline and proxyphylline contents (mg/tablet) and their corresponding confidence intervals at α=0.05, obtained by applying kinetic-spectrophotometric method (n = 18) and HPLC (n=9) to the pharmaceutical.

Method	Dyphylline	Proxyphylline	Theophylline
PLS1[a]	113.5 ± 4.7	117.1 ± 2.4	73.1 ± 1.0
HPLC	113.8 ± 1.3	114.0 ± 1.6	71.2 ± 1.6
Stated concentrations	112.5	112.5	75.0

[a]Wavelength range = 350-410; 470-550 nm; 6 PLS components for dyphylline and proxyphylline; and 2 for theophylline.

4. CONCLUSIONS.

As can be seen in this work, the joint use of multivariable calibration techniques and kinetic methods provides a powerful analytical tool for the simultaneous determination of very similar species presents in a commercial pharmaceutical. The kinetic-spectrophotometric method proposed allows the quantification without the previous extraction step necessary in HPLC.

5. ACKNOWLEDGEMENTS

The authors are grateful to Spain's DGICyT for funding this research within the framework of Projects PB97-0213 and PB96-1180. M. Porcel wishes to acknowledge additional support from the Spanish Ministry of Education and Science in the form of an FPI grant.

6. REFERENCES.

1. S. R. Crouch, A. Scheeline, E. S. Kirkor, *Anal. Chem.*, 2000, **72**, 53R.
2. T. F. Cullen, S. R. Crouch, *Mickrochim. Acta*, 1997, **126**, 1.
3. G. M. Ridder, D. W. Margerum, *Anal. Chem.*, 1979, **49**, 2090.

4. A. Cladera, E. Gómez, J. M. Estela, V. Cerdà, J. L. Cerdà *Anal. Chim. Acta*, 1993, **272**, 339.
5. J. M. Estela, A. Cladera, V. Cerdà *Anal. Chim. Acta*, 1995, **310**, 307.
6. B. M. Quencer, S. R. Crouch, *Anal. Chem*. 1994, **66**, 458.
7. S. M. Sultan, A. D. Walmsley, *Analyst*, 1997, **122**, 1601.
8. Y. Z. Ye, H. Y. Mao, Y. H. Chen, *Talanta*, 1998, **45**, 1123.
9. H. Martens and T. Naes, *Multivariate Calibration*, Wiley, New York, 1989.
10. M. Blanco, J. Coello, H. Iturriaga, S. Maspoch, M. Redón, *Anal. Chim. Acta*, 1995, **303**, 309.
11. M. Blanco, J. Coello, H. Iturriaga, S. Maspoch, M. Redón, *Anal. Chem.*, 1995, **67**, 4477.
12. M. Blanco, J. Coello, H. Iturriaga, S. Maspoch, M. Redón, J. F. Rodríguez, *Quim. Anal.*, 1996, **15**, 266.
13. M. Blanco, J. Coello, H. Iturriaga, S. Maspoch, M. Redón, N. Villegas, *Analyst*,1996, **121**, 395.
14. D. Pérez-Bendito, *Analyst*, 1990, **115**, 689.
15. T. Kappes, G. López-Cueto, J. F. Rodríguez-Medina, C. Ubide, *Analyst*, 1998, **123**, 2071.
16. T. F. Cullen, S. R. Crouch, *Anal. Chim. Acta*, 2000, **407**, 135.
17. S. R. Crouch, J. Coello, S. Maspoch, M. Porcel, *Anal. Chim. Acta*, 2000, **424**, 115.
18. M. Blanco, J. Coello, H. Iturriaga, S. Maspoch, J. Riba, *Anal. Chem.*, 1994, **66**, 2905.
19. M. Blanco, J. Coello, H. Iturriaga, S. Maspoch, M. Porcel, *Anal. Chim. Acta*, 2001, **431**, 115.
20. M. Blanco, J. Coello, H. Iturriaga, S. Maspoch, M. Porcel, *Anal. Chim. Acta*, 1999, **398**, 83.
21. I. Durán, A. Espinosa, F. Salinas, *Analyst*, 1995, **120**, 2567.
22. E. Martín, A. I. Jiménez, O. Hernández, F. Jiménez, J. J. Arias, *Talanta*, 1999, **49**, 143.
23. K. D. Khalaf, A. Morales-Rubio, M. De la Guardia, J. M. García, F. Jiménez, J. J. Arias, *Microchem J.*, 1996, **53**, 461.

24. G. López-Cueto, S. Maspoch, J. F. Rodríguez-Medina, C. Ubide, *Analyst*, 1996, **121**, 407.
25. J. M. García, A. I. Jiménez, J. J. Arias, K. D. Khalaf, A. Morales-Rubio, M. De la Guardia, *Analyst*, 1995, **120**, 313.
26. M. De la Guardia, K. D. Khalaf, B. A. Hasan, A. Morales-Rubio, J. J. Arias, J. M. García-Fraga, A. I. Jiménez, F. Jiménez, *Analyst*, 1996, **121**, 1321.
27. P. Depovere, M. Piraux, T. Adzet, *Circ. Farm.* 1975, **33**, 623.
28. J. C. Chiarino, *Anales Asoc. Quím. y Farm. Uruguay*, 1951, **51**, 13.
29. H. Raber, *Sci. Pharm.*, 1964, **32**, 122.
30. R. Ott, H. Wittmann-Zinke, *Sci. Pharm.*, 1958, **26**, 217.
31. M. M. Scotti, *Boll. Chim. Farm.*, 1965, **104**, 356.
32. S. R. El-Shabouri, S. A. Hussein, S. E. Emara, *Talanta*, 1989, **36**, 1288.
33. R. Pohloudek-Fabini, G. Döge, D. Kottke, *Pharmazie*, 1984, **39**, 24.
34. G. Peinhardt, *Pharmazie*, 1991, **46**, 812.
35. H. Iturriaga, J. Coello, S. Maspoch, M. Porcel, *Analyst*, *in press*.
36. M. Wenk, B. Eggs, F. Follath, *J. Chromatogr*., 1983, **276**, 341.

LISTA DE ABREVIATURAS

ADH	Alcohol deshidrogenasa.
ALS	*Alternating Least Squares*.
ANN	Redes neuronales artificiales (*Artificial Neural Networks*).
AO	Alcohol oxidasa.
BHA	Butilhidroxianisol.
BHT	Butilhidroxitolueno.
CAR	Adición continua de reactivo (*Continuous Addition of Reagent*).
CCDs	*Charge-coupled devices.*
CD o DC	Dicroísmo circular (*Circular Dichroism*).
CIDs	*Charge-injection devices.*
CLS	Regresión por mínimos cuadrados clásica (*Classical Least Squares*).
CPC	Cloruro de cetiltrimetilpiridina.
CR	Regresión continua (*Continuum Regression*).
CTAB	Bromuro de cetiltrimetilamonio.
EDTA	Ácido etilendiaminotetraacético.
FIA	Análisis por inyección de flujo (*Flow Injection Analysis*).
ILS	Regresión lineal múltiple inversa (*Inverse Least Squares*).
MBTH	3-metilbenzotiazolin-2-ona.
MLF	*Multi-Layer Feed-fordward Network.*
MLR	Regresión lineal múltiple.
MSE	Error cuadrático medio (*Mean Squared Error*).

MSECV Error cuadrático medio por *cross validation*.

NAS Señal neta del analito (*Net Analyte Signal*).

NIPALS *Nonlinear Iterative Partial Least Squares*.

N-PLS o

nPLS Regresión parcial por mínimos cuadrados multidimensional o multi-lineal (*Multilinear PLS*).

NQS 1,2-naftoquinona-4-sulfonato.

PAL Piridoxal.

PALP Fosfato-5'-piridoxal.

PAR 4-(2-piridilazo)resorcinol.

PARAFAC *Parallel factor analysis.*

PCA Análisis en componentes principales (*Principal Component Analysis*).

PCR Regresión en componentes principales (*Principal Component Regression*).

PCs Número de componentes principales.

PG Galato de propilo.

PLS Regresión parcial por mínimos cuadrados (*Partial Least Squares Regression*).

PRESS Suma de los cuadrados de los residuales de predicción (*Predicted Residual Error Sum of Squares*).

RMESC Raíz cuadrada del error cuadrático medio de calibración (*Root Mean Squared Error of Calibration*).

RMS(E) Raíz cuadrada del error cuadrático medio (*Root Mean Squred Error*).

RMSEC Raíz cuadrada del error cuadrático medio de calibración (*Root Mean Squred Error of Calibration*).

RMSEEP Raíz cuadrada del error cuadrático medio de predicción externa (*Root Mean Squared Error of External Prediction*).

RMSEP Raíz cuadrada del error cuadrático medio de predicción (*Root Mean Squred Error of Prediction*).

RSD(%) Desviación estándar relativa (*Relative Standard Deviation*).

RSE Error estándar relativo (*Relative Standard Error*).

RSEC Error estándar relativo de calibración (*Relative Standard Error of Calibration*)

RSEP Error estándar relativo de calibración (*Relative Standard Error of Prediction*)

SDBR Desviación estándar entre replicados (*Standard Deviation Between Replicates*).

SEP Error estándar de predicción (*Standard Error of Prediction*).

SVD Descomposición en valores singulares (*Singular Value Decomposition*).

TLD Descomposición trilineal (*Trilinear Decomposition*).

Todo trabajo realizado con placer no es completo si no se ofrece en dedicatoria. Y las dedicatorias siempre van dirigidas hacia aquellos que han hecho posible en mayor o en menor medida dicho trabajo. Por tanto, esta memoria va especialmente dedicada a todos los que han colaborado y me han apoyado, porque sin su intervención no hubiese logrado esta meta.